Progress In Electromagnetics Research, PIER 16, 205–225, 1997

ASSESSMENT OF THE EFFECTIVENESS OF ITERATIVE TECHNIQUES FOR THE EVALUATION OF THE ELECTROMAGNETIC SCATTERING BY WEAKLY NONLINEAR DIELECTRIC CYLINDERS

S. Caorsi

Department of Electronics
University of Pavia
Via Abboategrassp 209, I-27100, Pavia
Italy

A. Massa and M. Pastorino

Department of Biophysical and Electronic Engineering
University of Genoa
Via Opera Pia 11a, I-16145, Genova
Italy

1. INTRODUCTION

This paper aims to evaluate the effectiveness of iterative numerical approaches to the computation of the electromagnetic scattering by weakly nonlinear dielectric infinite cylinders in free space and to compare such approaches. The cylinders are assumed to be nonmagnetic, inhomogeneous and of arbitrary shapes. A time-periodic transverse-magnetic illumination is assumed [1] that reduces the problem to a scalar one, under the assumption that the nonlinearity is such as not

to modify the scalar nature of the dielectric permittivity. Both the electromagnetic field and the bistatic scattering width (which gives the behavior of the scattered electric field at a large distance from the scatterer) are computed starting from an integral-equation formulation previously developed in [2–3] for quite a different problem, i.e., field prediction in 3D scattering, for which an *exact* numerical solution was exploited. In this context, the term *exact* means that no approximations are considered for the solution, apart from the one related to the weakness of the nonlinearity (which allows one to perform series truncations) and those related to the numerical discretization. Under these hypothesis, the mentioned formulation provides formal solutions for the scattered electric fields at the fundamental frequency and at higher-order frequencies, taking into account (by means of coupling terms) the contributions of the interactions between the generated harmonic components. By truncating the series expansion of the e.m. field at a suitable term and by discretizing the continuous problem, we obtain a nonlinear system of algebraic equations to be solved for the complex harmonic amplitudes of the electric field vector. The solution of this system is critical, and the approach presented in [2–3] did not address the resulting numerical problem in an adequate way. In [4], the problem solution was reduced to the minimization of a multivalue multivariable function. In order to find a global minimum for the resulting *energy* function, we used a statistical-cooling procedure.

In this paper, for weakly nonlinear scatterers, different approaches to the problem solution are taken. In particular, iterative approaches are considered that compute the scattering quantities by using the so-called distorted-wave Born approximation (widely applied for linear inverse scattering problems [5]), and, in simplified versions, the first-order Born approximation [6] and the Rytov approximation [7–8]. The Born approximation was previously applied in [9] in the case of infinite cylinders of circular cross-sections. To assess the reliability of the obtained results, they are compared with those obtained by the *exact* solution [4]. In the following, the mathematical formulation for the iterative approaches is outlined; then the methodologies are applied to several examples, concerning circular cylinders as well as scatterers with irregular cross-sections. Comparisons are made in terms of a suitable error parameter and the field predictions under different conditions are reported. In particular, the scattering computation is evaluated for different nonlinearities, for different values of the linear

parameters and for different dimensions of the scatterers in terms of the wavelength of the incident wave.

2. DESCRIPTION OF THE METHOD

Let S be the cross-section of an infinite cylinder with the cylindrical axis parallel to the z axis. Let $\mathbf{E}^i(\mathbf{r},t) = \Psi^i_z(\mathbf{r},t)\mathbf{z}$, $\mathbf{r} = (x,y)$, be a transverse magnetic incident wave polarized along the z axis and impinging normally on the cylinder. The total electric field is denoted by $\mathbf{E}(\mathbf{r},t) = \Psi_z(\mathbf{r},t)\mathbf{z}$ and the subscript z will be omitted in the following.

In this paper, we assume the dielectric permittivity to be dependent on the internal electric field through the relation:

$$\varepsilon_{NL}(\mathbf{r},t) = \varepsilon_0[\varepsilon_L(\mathbf{r}) + NL(\mathbf{E}(\mathbf{r},t))] \tag{1}$$

where $\varepsilon_L(\mathbf{r})$ is the linear part and $NL(\Psi(\mathbf{r},t))$ is an operator (responsible for the nonlinearity) which does not modify the scalar nature of the dielectric permittivity and produces a time-periodic output, under the aforesaid hypothesis on the illuminating field. The scatterer cross-section is inhomogeneous both due to the nonlinearity and in the limit $\mathbf{E}(\mathbf{r},t) \to 0$ [11]. According to [2], after expanding $\Psi(\mathbf{r},t)$, $\Psi^i(\mathbf{r},t)$, and $NL(\Psi(\mathbf{r},t))$ in Fourier series at the fundamental frequency $f_0 = \omega_0/2\pi$ in the case of weak nonlinearities, the following inhomogeneous wave equation holds for each harmonic component:

$$[\nabla_t^2 + k_m^2]\Psi^{s(m)}(\mathbf{r}) = -k_m^2(\varepsilon_L(\mathbf{r}) - 1)\Psi^{(m)}(r) - k_m^2\Omega^{(m)}(\mathbf{r}) \tag{2}$$

where $k_m^2 = m^2\omega_0^2\varepsilon_0\mu_0$, and $\Psi^{s(m)}(\mathbf{r})$ is the m^{th} harmonic component of the scattered electric field, and is given by: $\Psi^{s(m)}(\mathbf{r}) = \Psi^{(m)}(\mathbf{r}) - \Psi^{i(m)}(\mathbf{r})$, where $\Psi^{(m)}(\mathbf{r})$ and $\Psi^{i(m)}(\mathbf{r})$ are the m^{th} harmonic components of $\Psi(\mathbf{r},t)$ and $\Psi^i(\mathbf{r},t)$. The term $\Omega^{(m)}(\mathbf{r})$ is a coupling term dependent on the field components at the same frequency and at other frequencies; it is given by [2]:

$$\Omega^{(m)}(\mathbf{r}) = \sum_{i=-\infty}^{\infty}\sum_{j=-\infty}^{\infty} \kappa_{ij}^m \Theta_i(\mathbf{r})\Psi^{(j)}(\mathbf{r}) \tag{3}$$

where $\kappa_{ij}^m = 1$, if $i + j = m$, and $\kappa_{ij}^m = 0$, otherwise. $\Theta_i(x,y)$ is the i^{th} harmonic component of $NL(\Psi(\mathbf{r},t))$. The coupling term

$\Omega^{(m)}(\mathbf{r})$ can be rendered explicitly, once the nonlinear operator has been specified.

In this paper, we aim to reach iterative approximate solutions to (2). First, a solution is achieved by applying the distorted-wave Born approximation [5], which expresses the scattered electric field in terms of an internal field that would be present in the linear case $(NL(\Psi(\mathbf{r},t)=0))$. If we apply this approximation, we can express the scattered electric field (for $m=1$) in terms of the linear internal field. We obtain:

$$\begin{aligned}\Psi^{(1)}(\mathbf{r}) = \Psi^{i(1)}(\mathbf{r}) &- j(k_1^2/4)\int_S (\varepsilon_L(\mathbf{r}')-1)\Psi^L(\mathbf{r}')H_o^{(2)}(k_1\rho)d\mathbf{r}' \\ &- j(k_1^2/4)\int_S \Omega^{L-(1)}(\mathbf{r}')H_o^{(2)}(k_1\rho)d\mathbf{r}'\end{aligned} \tag{4}$$

where $\Psi^L(\mathbf{r})$ is the field that would be present in a cylinder with a homogeneous permittivity equal to the linear part of the actual permittivity; $H_o^{(2)}(k_1\rho)$ is the Hankel function of the second kind and the zero-th order, and ρ is given by: $\rho = |\mathbf{r}-\mathbf{r}'|$. In relation (4), the superscript in the term $\Omega^{L-(1)}(\mathbf{r})$ indicates that the coupling term is computed by (3) in terms of the linear field $\Psi^L(\mathbf{r})$. The bistatic scattering width, $W_{2-D}(\phi)$ is also introduced, which is defined as [10]:

$$W_{2-D}(\phi) = \lim_{\rho\to\infty}\left[2\pi\rho\frac{|\mathbf{E}^s(\rho,\phi)|^2}{|\mathbf{E}^i(\rho,\phi)|^2}\right] \tag{5}$$

where ρ and ϕ denote the cylinder coordinates related to x and y: $\rho=\sqrt{(x^2+y^2)}$ and $\phi=\tan^{-1}(y/x)$.

The generated higher-order harmonics $(m=2,\ldots)$ are obtained by the equation:

$$\Psi^{(m)}(\mathbf{r}) = -j(k_m^2/4)\int_S \Omega^{L-(m)}(\mathbf{r}')H_o^{(2)}(k_m\rho)d\mathbf{r}' \tag{6}$$

Simpler approximate solution to equations (4) and (6) can be obtained by using the classic first-order Born approximation, in which the internal total electric field is approximated by the known incident field [6]:

$$\begin{aligned}\Psi^{(1)}(\mathbf{r}) = \Psi^{i(1)}(\mathbf{r}) &- j(k_1^2/4)\int_S (\varepsilon_L(\mathbf{r}')-1)\Psi^{i(1)}(\mathbf{r}')H_o^2(k_1\rho)d\mathbf{r}' \\ &- j(k_1^2/4)\int_S \Omega^{B-(1)}(\mathbf{r}')H_o^{(2)}(k_1\rho)d\mathbf{r}'\end{aligned} \tag{7}$$

$$\Psi^{(m)}(\mathbf{r}) = -j(k_m^2/4)\int_S \Omega^{B-(m)}(\mathbf{r}')H_o^2(k_m\rho)d\mathbf{r}' \tag{8}$$

where $\Omega^{B-(m)}(\mathbf{r})$ indicates that the coupling term is computed by using (3), on the basis of the incident field only.

The third approach is developed by using the Rytov approximation. This approximation allows variations in the complex phase $\Phi^{s(1)}(\mathbf{r})$ inside S to be neglected, $\Phi^{s(1)}(\mathbf{r})$ being such that $\Psi^{(1)}(\mathbf{r}) = \exp\{\Phi^{s(1)}(\mathbf{r}) + \Phi^{i(s)}(\mathbf{r})\}$, with $\Phi^{i(1)}(\mathbf{r})$ given by $\Psi^{i(1)}(\mathbf{r}) = \exp\{\Phi^{i(1)}(\mathbf{r})\}$ [7]. By applying the RA, which is essentially an approximation concerning the phase of the field [7], we obtain

$$\begin{aligned}\Phi^{s(1)}(\mathbf{r}) = \frac{-1}{\Psi^{i(1)}(\mathbf{r})}\Bigg[&j(k_1^2/4)\int_S(\varepsilon_L(\mathbf{r}')-1)\Psi^{i(1)}(\mathbf{r}')H_o^{(2)}(k_1\rho)d\mathbf{r}' \\ &+j(k_1^2/4)\int_S \Omega^{R-(1)}(\mathbf{r}')H_o^{(2)}(k_1\rho)dr'\Bigg]\end{aligned} \tag{9}$$

where $\Omega^{R-(1)}(\mathbf{r})$ indicates that the coupling term is computed by using (3), within the Rytov approximation. The generated higher order-harmonic components are then computed by relations analogous to those used for the other approximate approaches.

In order to develop iterative processes for the computation of the electric field distributions inside and outside S, we assume that the nonlinear field at step $(k+1)$, $\Psi_{k+1}^{(m)}(\mathbf{r})$, is given by (4) and (6), (7)–(8) or (9), in which the integrals are computed in terms of the field at step k (including the coupling terms $\Omega_k^{X-(1)}(\mathbf{r})$, $X = L, B, R$). The equations describing the iterative processes can be found in references [8] and [9].

The convergence of each proposed iterative approach is evaluated by means of the following residual error:

$$\begin{aligned}\Re\{k+1\} =& S^{-1}\int_S\Bigg\{\Psi_{k+1}^{(1)}(\mathbf{r}') - \Psi^{i(1)}(\mathbf{r}') \\ &+ j(k_1^2/4)\int_S[\varepsilon_L(\mathbf{s}')-1]\Psi_{k+1}^{t(1)}(\mathbf{s}')H_o^{(2)}(k_1\xi)d\mathbf{s}' \\ &+ j(k_1^2/4)\int_S \Omega_{k+1}^{NL(1)}(\mathbf{s}')H_o^{(2)}(k_1\xi)d\mathbf{s}'\Bigg\}d\mathbf{r}'\end{aligned} \tag{10}$$

where $\xi = |\mathbf{r}' - \mathbf{s}'|$. A given approach is assumed to be convergent if $\Re\{k\} \to 0$, as $k \to \infty$. In order to apply the distorted-wave Born

approximation, at the first iteration step, the field $\Psi^L(\mathbf{r}')$ is numerically computed by the Richmond formulation [12], which has been proved to be accurate for forward-scattering by dielectric cylinders, if a TM illumination is used. The cross-section S is partitioned into P subdomains, $p = 1, \ldots, P$, and the field and dielectric parameters are assumed to be constant inside each cell. The problem solution can be obtained by the matrix equation:

$$[Z]\underline{\Psi}^L = \underline{\Psi}^i \tag{11}$$

where $\underline{\Psi}^L$ the unknown array (dimensions: $P \times 1$), whose elements are given by: $\psi_p^L = \Psi^L(\mathbf{r}_p)$, $p = 1, \ldots, P$, where $\mathbf{r}_p$ is the center of the p^{th} subdomain; $\underline{\Psi}^i$ is the known term $(P \times 1)$, whose elements are given by: $\psi_p^i = \Psi^{i(1)}(\mathbf{r}_p)$, $p = 1, \ldots, P$; $[Z]$ is the impedance matrix $(P \times P)$, whose generic elements are $z_{pq} = (j/2)[\varepsilon_L(\mathbf{r}_p) - 1][\pi k_1 a_p H_1^{(2)}(k_1 a_p) - 2j]$ if $p = q$, and $z_{pq} = (j/2)[\varepsilon_L(\mathbf{r}_p) - 1]\pi k_1 a_p J_1(k_1 a_p) H_o^{(2)}(k_1 \rho_{pq})$ if $p \neq q$, where $\rho_{pq} = |\mathbf{r}_p - \mathbf{r}_q|$ and $a_p = (S_p/\pi)^{1/2}$, S_p being the area of the p^{th} subdomain.

In the paper, we place emphasis on the scattering width (related to the fundamental field components). Moreover, some examples, concerning the field distributions at the fundamental component as well as at the third harmonic component will be given in the following section.

3. NUMERICAL RESULTS

In the first set of numerical simulations, we considered the scattering by an infinite cylinder with a circular cross-section. The nonlinearity was assumed to be of the Kerr type, for which relation (1) can be rewritten as:

$$\varepsilon_{NL}(\mathbf{r}, t) = \varepsilon_0[\varepsilon_L(\mathbf{r}) + \beta|\Psi(\mathbf{r}, t)|^2] \tag{12}$$

As a consequence of this choice, the coefficients $\Omega^{(m)}(x, y)$ in (3) can now be rendered explicitly. They are given by:

$$\Omega^{(m)}(\mathbf{r}) = \beta T^{-1} \int_T \Psi(\mathbf{r}, t)^2 e^{-jm\omega_0 t} dt \tag{13}$$

where $T = 2\pi/\omega_0$. In the first example, we assumed a unit uniform monochromatic plane wave propagating along the x axis. Moreover, the cross-section of the cylinder was assumed to be homogeneous in

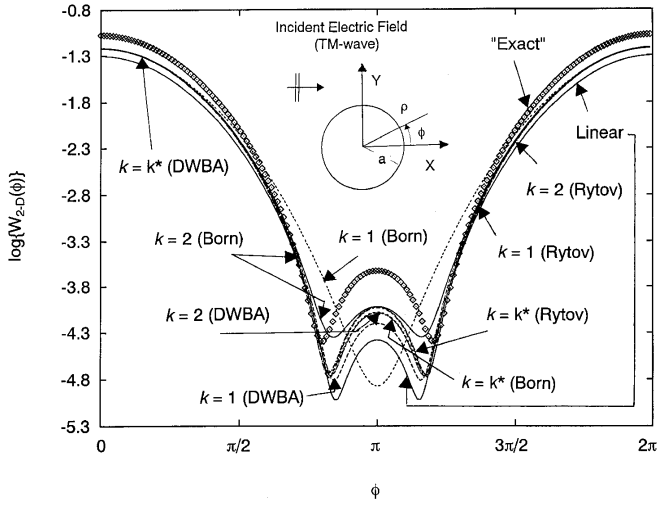

Figure 1. Bistatic scattering width of a NL circular cylinder ($k_1 a = 0.6\pi$; $\varepsilon_L = 1.1$, $P = 225$, $\beta = 0.01$). Linear and nonlinear values obtained by the statistical cooling procedure (*exact* solution) and the iterative techniques (DWBA, Born approximation, and Rytov approximation).

its linear part ($\varepsilon_L(\mathbf{r}) = \varepsilon_L = 1.1$) and with a radius a such that $k_1 a = 0.6\pi$. The other assumed parameters were: $\beta = 0.01$ and $P = 225$. The partitioning of the cross-section was made according to the rule proposed in [9], where the circular cross-section was partitioned into shells and each shell was divided into subareas by radial segments. If each subarea had the same area as the innermost (circular) layer, the number of subareas of each shell turned out to be an integer number. Figure 1 shows the computed values of the bistatic scattering width, obtained by using the distorted-wave Born approximation, the Born approximation, the Rytov approximation, and the *exact* (numerical) solution [4]. The values of the linear bistatic scattering width analytically computed are also provided for comparison. The main objective of this example is to evaluate the capabilities of the iterative approaches versus the statistical cooling solution. However, it is worth noting that, only for circular cylinders, results obtained by the distorted-wave Born approximation have already been compared in [9] with those obtained by Hasan and Uslenghi [13] by using a per-

turbation method and with those obtained by Censor [14] by using an iterative method. Figure 1 gives the values for $k = 1$, $k = 2$, and $k = k^*$ (this value of k turned out to be sufficient for the assumed *convergence*, i.e., at step k^* the residual error $\Re\{k^*\}$ turned out to be less than a fixed threshold value, $\Re_{\text{th}}$; in all the simulations, we assumed $\Re_{\text{th}} = 10^{-4}$). The analytically computed linear values are also reported. As can be seen from this figure, the nonlinearity is rather weak and the iterative approaches converge very fast. Moreover, rather an accurate prediction of the bistatic scattering width is obtained also at the first iteration step, except when the first-order Born approximation is used: in this case, at the first iteration step, significant errors are incurred, especially in the backscattering direction.

Figures 2(a) and 2(b) give the amplitudes of the total electric field at the fundamental frequency and at the third order harmonic computed along the x axis ($y = 0.0$). As a Kerr-like nonlinearity was used, the second-order harmonic is vanishing [13], and the third harmonic component was found to be the only significant one for weak nonlinearities. Similar conclusions to that drawn from Figure 1 can be deduced from Figure 2; the obtained results are in good agreement (especially inside the cylinder) with those obtained by the statistical cooling procedure. The above consideration is confirmed by Figures 3(a) and 3(b), which give the convergence values of the total electric fields at the centers of the discretization subdomains of the circular cross-section of the cylinder. According to the rule defined in [9], the polar coordinates of these points (c_p) are given by:

$$\begin{aligned} c_p &= (\rho, \phi) \\ &= \left\{ \lceil (p+6)/8 \rceil a_p,\ 2\pi [n - 2 - \lceil (p-2)/8 \rceil 8] \cdot [\lceil (p+6)/8 \rceil 8]^{-1} \right\} \\ c_1 &= (0,0) \qquad\qquad p = 2, \ldots, P \end{aligned} \tag{14}$$

where a_p is defined after equation (11) and the symbol "$\lceil \xi \rceil$" denotes the integer part of ξ.

In order to compare the obtained results, the following error parameter is defined:

$$\text{ERR}^{(m)}(\mathbf{r}) = \frac{\Psi^{(m)}_{\text{approx}}(\mathbf{r}) - \Psi^{(m)}_{\text{exact}}(\mathbf{r})}{\Psi^{(m)}_{\text{exact}}(\mathbf{r})} \tag{15}$$

where $\Psi^{(m)}_{\text{approx}}(\mathbf{r})$ denotes the m^{th} harmonic component of the total electric field computed at point $\mathbf{r}$ by using a given approximation

(specified in the figures), and $\Psi^{(m)}_{\text{exact}}(\mathbf{r})$ indicates the same quantity as computed by the statistical cooling procedure [4]. Figures 4(a) and 4(b) give the plots of $\text{ERR}^{(m)}(\mathbf{r})$, for $m = 1$ and $m = 3$, computed at the centers of the discretization subdomains.

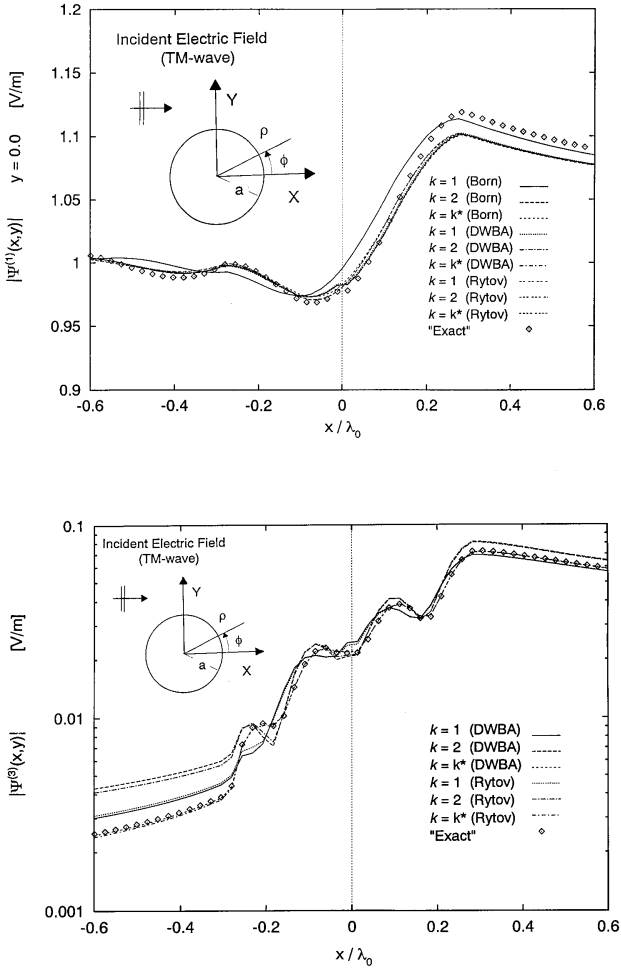

Figure 2. Scattering by a NL circular cylinder ($k_1 a = 0.6\pi$; $\varepsilon_L = 1.1$, $P = 225$, $\beta = 0.01$). (a) Amplitude of the fundamental harmonic component of the total electric field along the x axis. (b) Amplitude of the third harmonic component of the total electric field along the x axis.

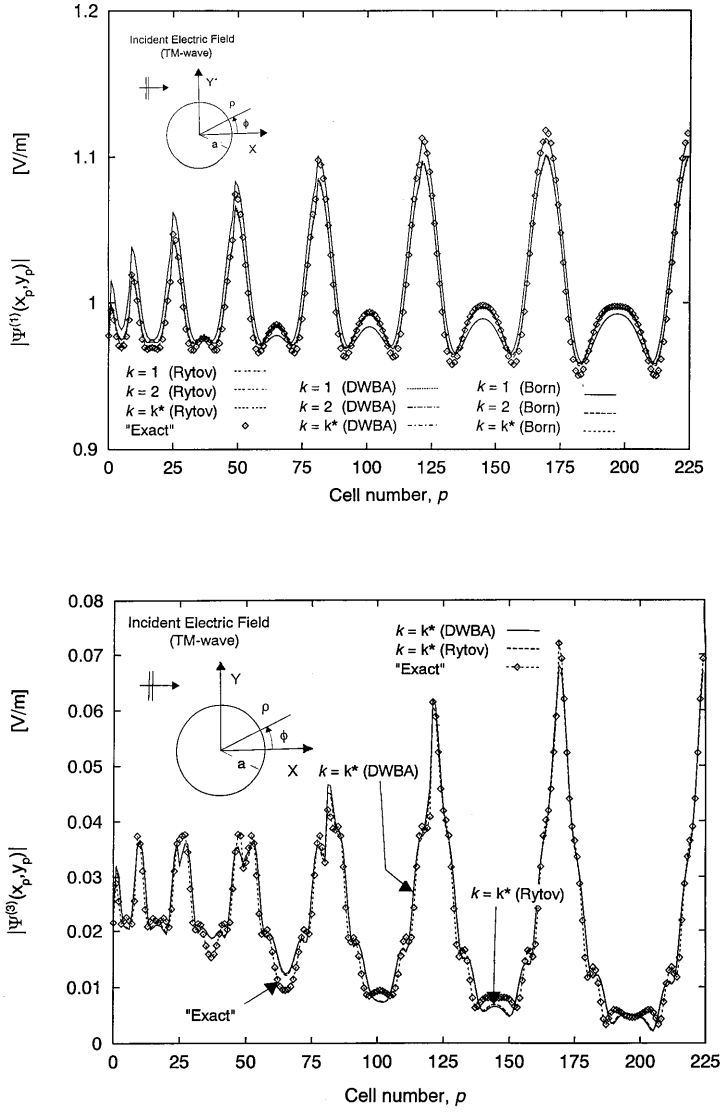

Figure 3. Scattering by a NL circular cylinder ($k_1 a = 0.6\pi$; $\varepsilon_L = 1.1$, $P = 225$, $\beta = 0.01$). (a) Amplitude of the first harmonic terms of the total electric fields computed at the centers of the discretization subdomains of the circular cylinder cross-section. (b) Amplitude of the third harmonic terms of the total electric fields computed at the centers of the discretization subdomains of the circular cylinder cross-section.

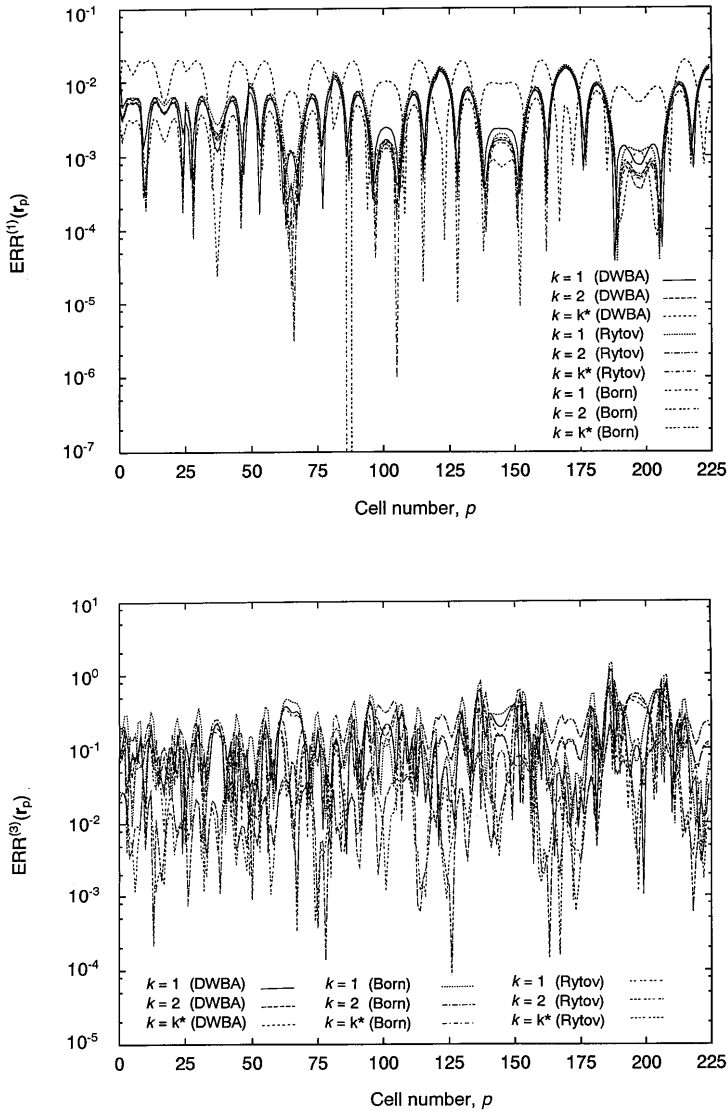

Figure 4. Iterative techniques: Values of the error parameter, $\mathrm{ERR}^{(m)}(r)$, for $m = 1$ (a) and $m = 3$ (b), computed at the centers of the discretization subdomains of NL circular cylinder in Fig. 3 ($k_1 a = 0.6\pi$; $\varepsilon_L = 1.1$, $P = 225$, $\beta = 0.01$).

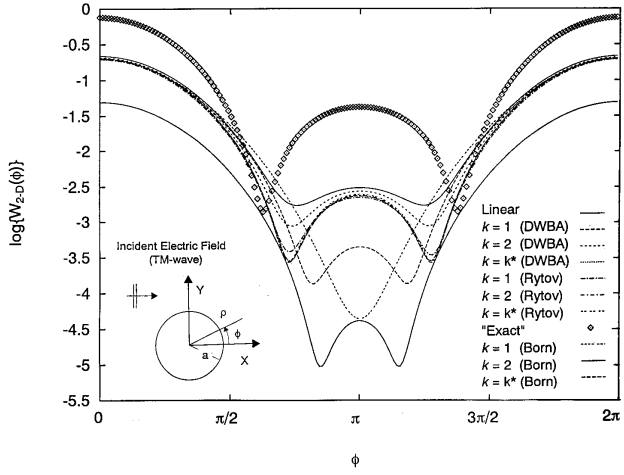

Figure 5. Bistatic scattering width of a NL circular cylinder ($k_1 a = 0.6\pi$; $\varepsilon_L = 1.1$, $P = 225$, $\beta = 0.1$). Linear and nonlinear values obtained by the statistical cooling procedure (*exact* solution) and the iterative techniques (DWBA, Born approximation, and Rytov approximation).

In the second example, the same circular scatterer is considered in the case in which the nonlinear parameter is assumed to be equal to $\beta = 0.1$ (corresponding to quite a significant nonlinearity). Figure 5 gives the bistatic scattering width. As can be noticed, in comparison with Figure 1, certain errors are incurred when the iterative approaches are applied, in both the forward and backscattering directions. The figure gives the errors incurred at the first two iterations and when the convergence had been reached ($k = k^*$). The linear values (analytically computed) are also provided. As can be seen, at the first iterations, large errors are present, especially if the Born and the distorted-wave Born approximations are used. For this case, the Rytov approximation at the first iteration step is more accurate. This can be justified by the fact that the scatterer has a permittivity with a low real part so that, even though the nonlinearity is rather significant, the effective dielectric permittivity given by relation (1) changes rather slowly (no marked discontinuities are present in the propagation medium). It has been proved that the Rytov approximation works better than the Born-type ones when this condition holds [15]. Analogous conclusions can be drawn from Figures 6(a) and 6(b), which give

the amplitudes of the convergence values of the total electric fields at the fundamental frequency and at the third harmonic component computed at the centers of the discretization subareas.

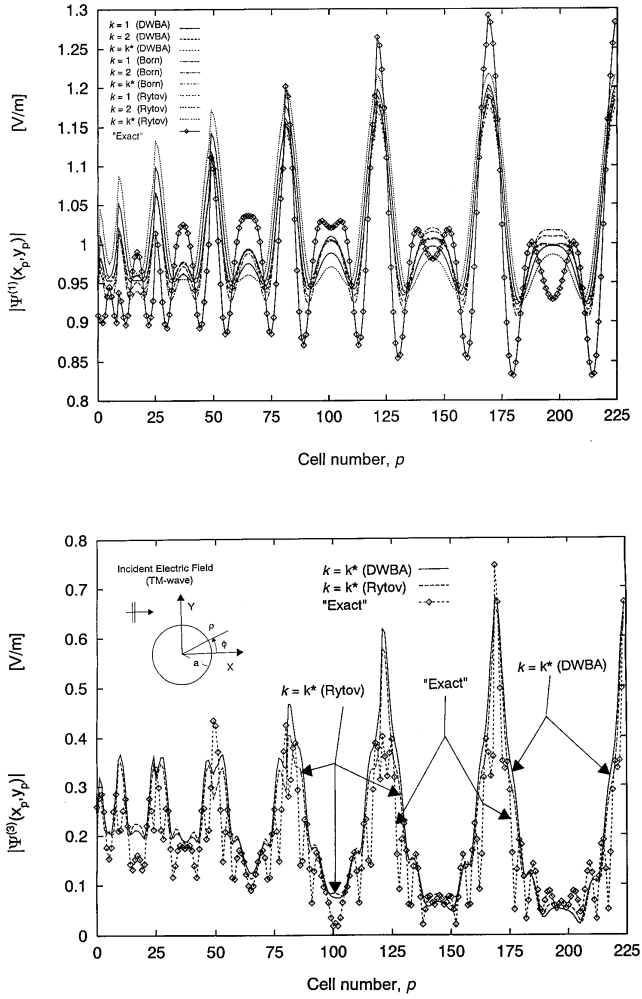

Figure 6. Scattering by a NL circular cylinder ($k_1 a = 0.6\pi$; $\varepsilon_L = 1.1$, $P = 225$, $\beta = 0.1$). (a) Amplitude of the first harmonic terms of the total electric fields computed at the centers of the discretization subdomains of the circular cylinder cross-section. (b) Amplitude of the third harmonic terms of the total electric fields computed at the centers of the discretization subdomains of the circular cylinder cross-section.

On the basis of the above considerations, let us now concentrate on the application of the Rytov approximation. The following parameters were used for the circular cylinder: $\varepsilon_L = 1.1$, $k_1 a = 2\pi$, $\beta = 0.1$ and $P = 225$. The scatterer was larger than the previous one in terms of the wavelength of the monochromatic incident field. Figures 7 and 8 give an idea of the behavior of the iterative process at different iteration steps and for different values of the nonlinear parameter. In particular, Figure 7 shows the values of the bistatic scattering width, obtained at steps $k = 1, \ldots, 10$. The linear values (analytically computed) are also provided. Figure 8 gives the values of the bistatic scattering width for the same scatterer for some significant values of the nonlinear parameter β. For $\beta < 0.2$, the iterative process is convergent and the values at step $k = k^*$ are provided. On the contrary, for $\beta \geq 0.2$, the iterative process is divergent and the values at $k = 1$ are provided. These values can be of some interest all the same, as the residual error defined in [9] turned out to be quite small at this iteration step when the Rytov approximation was used $(\Re\{k = 1\} < 0.20)$. It is also interesting to note the asymmetric behavior with respect to $\phi = \pi$. Such asymmetry is not physical and actually disappears (for greater values of k) when the process is convergent.

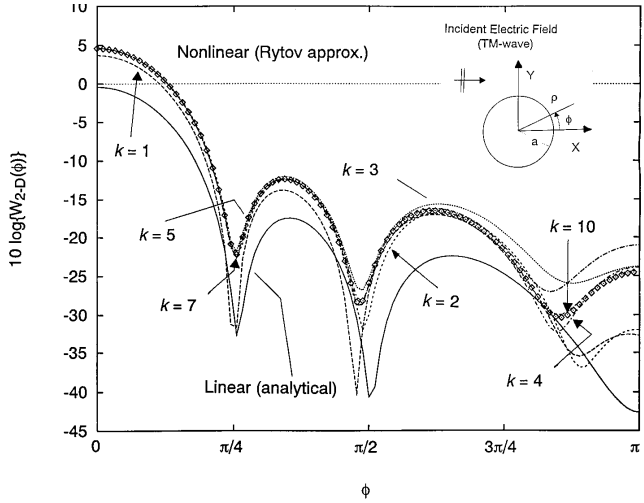

Figure 7. Rytov approximation, iterative process: bistatic scattering width of a NL infinite cylinder of circular cross-section ($k_1 a = 2\pi$; $\varepsilon_L = 1.1$, $P = 225$, $\beta = 0.1$). k: iteration number (RA).

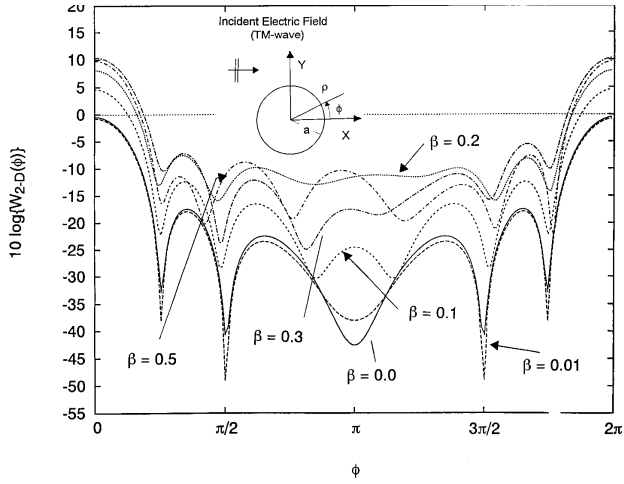

Figure 8. Effects of the nonlinear parameter β. Bistatic scattering width of a NL infinite cylinder of circular cross-section ($k_1 a = 2\pi$; $\varepsilon_L = 1.1,\ P = 225$) obtained by using the Rytov approximation (RA).

The numerical approach is applicable to cylinders of arbitrary cross-section shapes. So, in other simulations, a scatterer with an irregular cross-section was considered (Figure 9). The same incident field as in the previous example was assumed. The other parameters of the nonlinear cylinder were: $\varepsilon_L = 1.1$, $\beta = 0.01$ and $P = 145$ (uniformly spaced square cells). The linear dimensions of the cross-section are given in Figure 9 in terms of the wavelength of the incident monochromatic field, λ_0. This figure shows the values of the bistatic scattering width, obtained by using the distorted-wave Born approximation, the classic Born approximation, the Rytov approximation, and the *exact* solution [4]. The linear values (numerically computed by the Richmond method) are also provided. As can be seen, there is a good agreement between the convergence values obtained by the iterative approaches and the results of the statistical cooling procedure. Significant errors were incurred at the first iteration step in the backscattering direction when the Born approximation was used. The same conclusion can be drawn from Figure 10, which gives the total electric fields at the fundamental frequency and at the third-order harmonic. Moreover, for the generated third harmonic component, the Rytov approximation, even at convergence, predicted values a bit higher than that provided by the statistical cooling procedure in the forward direction. This is probably

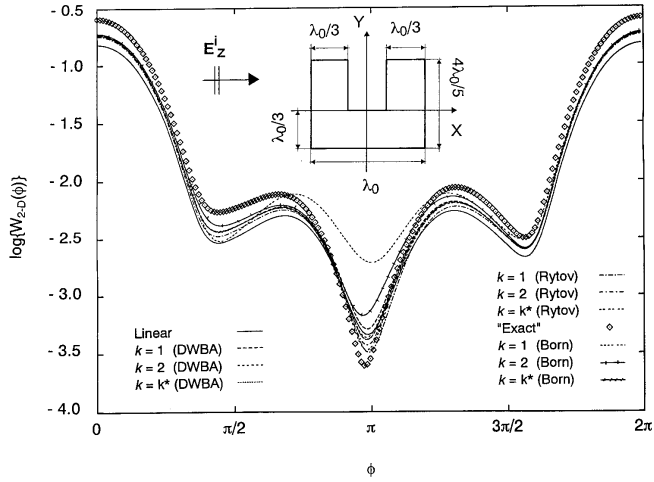

Figure 9. Bistatic scattering width of a NL dielectric cylinder of irregular cross-section ($\varepsilon_L = 1.1$, $P = 145$, $\beta = 0.01$). Linear and nonlinear values obtained by the statistical cooling procedure (*exact* solution) and the iterative techniques (DWBA, Born approximation, and Rytov approximation).

to be ascribed to the "multiple" interfaces encountered by the incident waves, which make the whole scatterer present more marked jumps in the dielectric parameters than the previous circular cylinder. The quantitative errors concerning the centers of the discretization subdomain are given in Figures 11(a) and 11(b) (parameter $\mathrm{ERR}^{(m)}(r)$, $m = 1$ and $m = 3$).

Finally, Figure 12 gives the values of the bistatic scattering width for another irregular scatterer, which was larger in terms of wavelength. Moreover, this scatterer exhibited a larger linear part of the dielectric permittivity: $\varepsilon_L = 1.5$. The other parameters were: $\beta = 0.01$ and $P = 135$ (uniformly spaced square cells). Even though the nonlinear parameter was small, the whole scatterer represented a stronger scatterer (as compared with the previous ones) for the various iterative approaches. In this case, the iterative processes based on the classic Born approximation and on the Rytov approximation were divergent, although, even in this case, the solutions at the first iteration ($k = 1$) can be of some interest for the same reasons as in the previous divergent

case. The prediction of the bistatic scattering width was rather accurate in the forward direction; on the contrary, in the backscattering direction, significant errors were present.

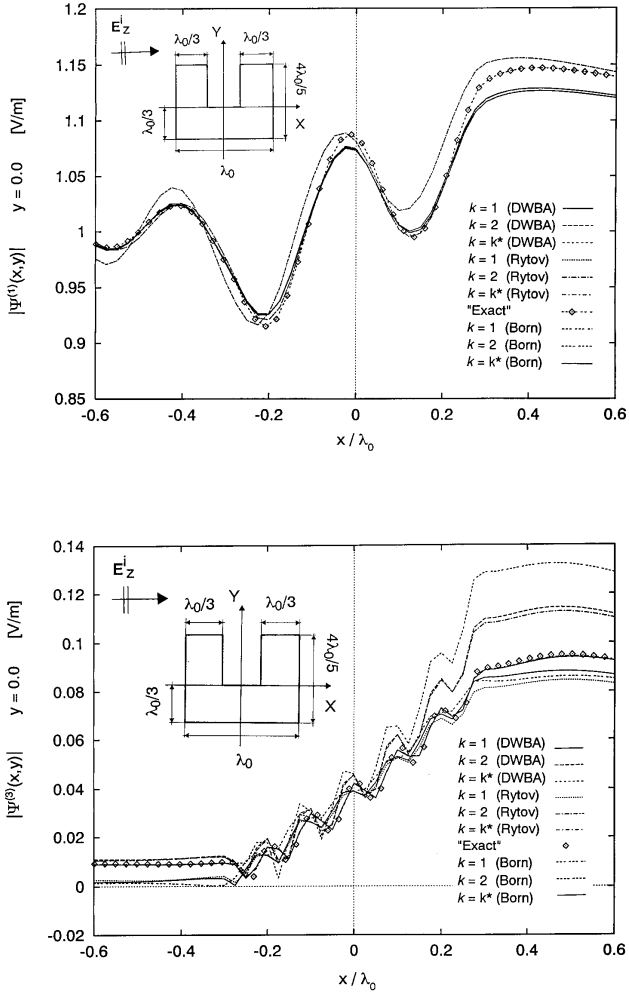

Figure 10. Scattering by a NL cylinder of irregular cross-section ($\varepsilon_L = 1.1,\ P = 145,\ \beta = 0.01$). (a) Amplitude of the fundamental harmonic component of the total electric field along the x axis. (b) Amplitude of the third harmonic component of the total electric field along the x axis.

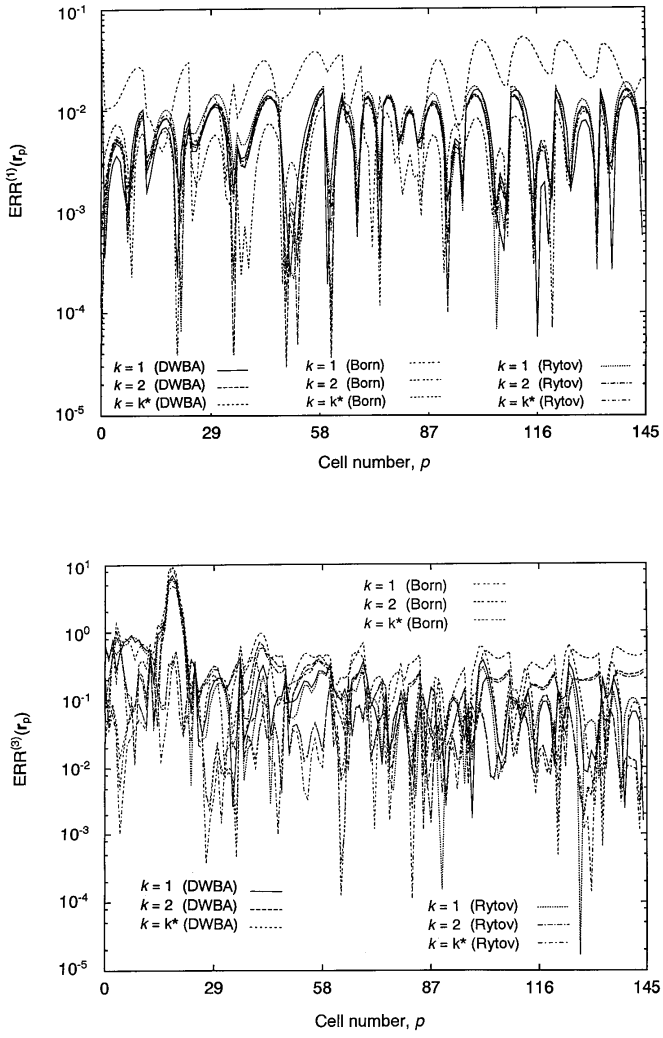

Figure 11. Iterative techniques: Values of the error parameter, $\mathrm{ERR}^{(m)}(r)$, for $m = 1$ (a) and $m = 3$ (b), computed at the centers of the discretization subdomains of NL cylinder of irregular cross section in Fig. 10 ($\varepsilon_L = 1.1,\ P = 145,\ \beta = 0.01$).

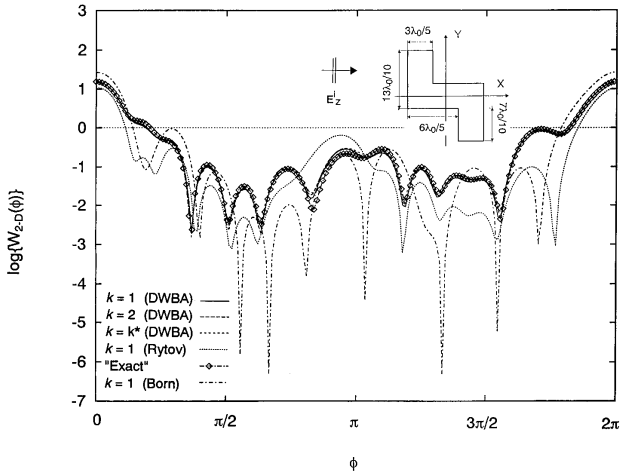

Figure 12. Bistatic scattering width of an infinite NL dielectric cylinder of irregular cross section ($\varepsilon_L = 1.1,\ P = 135,\ \beta = 0.01$). Linear and nonlinear values obtained by the statistical cooling procedure (*exact* solution) and iterative techniques (DWBA, Born approximation, and Rytov approximation).

4. CONCLUSIONS

In the paper, some iterative approaches to the approximate computations of the scattering widths of nonlinear cylinders of arbitrary shapes have been evaluated. The approaches make use of the distorted-wave Born approximation and, in simpler versions of the method, the Born approximation and the Rytov approximation are applied. The paper has described the scattering by several cylinders (isotropic, lossless and nonmagnetic) of various cross-section shapes. The results have been compared with those obtained by using a solution based on a statistical cooling procedure. The electric fields, both inside and outside the scatterers, and the bistatic scattering widths have been computed. The obtained values have been evaluated in terms of a defined quantitative error. The results show that, as long as a scatterer is weak with respect to the propagation medium (i.e., the nonlinearity and the linear part of the dielectric permittivity are small), the iterative solutions can accurately predict the electromagnetic scattering, taking into account the generation of higher-order harmonics and the effects of these generated harmonics on the field at the fundamental frequency.

REFERENCES

1. Stratton, J. A., *Electromagnetic Theory.* New York, McGraw-Hill, 1941.
2. Caorsi, S., A. Massa, and M. Pastorino, "A numerical solution to full-vector electromagnetic scattering by 3D nonlinear bounded dielectrics," *IEEE Trans. Microwave Theory Tech.*,Vol. 43, 428–436, 1995.
3. Caorsi, S., A. Massa, and M. Pastorino, "Extension of moment-method solutions to vector scattering by three-dimensional nonlinear dielectric objects in free space," *International Journal for Numerical Methods in Engineering*, Vol. 38, 809–821, 1995.
4. Caorsi, S., A. Massa, and M. Pastorino, "Optimization procedure based on a statistical cooling method applied to scattering by bounded nonlinear objects," *Radio Science*, Vol. 31, 437–450, 1996.
5. Wombell, R. J., and R. D. Murch, "The reconstruction of dielectric objects from scattered field data using the distorted-wave Born approximation," *J. Electromagn. Waves Applic.*, Vol. 7, 687–702, 1993.
6. Morse, P. M., and H. Feshbach, *Methods of Theoretical Physics*, McGraw-Hill, New York, 1953.
7. Kaveh, M., M. Soumekh, and R. K. Mueller, "A comparison of Born and Rytov approximations in acoustic tomography," in *Acoustical Imaging*, Vol. 11, J. P. Power (Ed.). New York: Plenum, 1982.
8. Caorsi, S., A. Massa, and M. Pastorino, "The Rytov approximation: application to scattering by two-dimensional weakly nonlinear dielectrics," *J. Opt. Soc. Am. A*, (in press).
9. Caorsi, S., A. Massa, and M. Pastorino, "Approximate solutions to the scattering by nonlinear isotropic cylinders of circular cross-sections," *IEEE Trans. Antennas Propagat.*, Vol. 43, 1262–1269, 1995.
10. Balanis, C. A., *Advanced Engineering Electromagnetics*, New York, John Wiley & Sons, 1989.
11. Miyagi, M., and S. Nishida, "Guided waves in bounded nonlinear medium (II). Dielectric boundaries," *Sci Rep. Res. Inst. Tohoku Univ. B (Electron. Commun.)*, Vol. 24, 53–67, 1972.
12. Richmond, J. H., "Scattering by a dielectric cylinder of arbitrary cross-section shape," *IEEE Trans. on Antennas Propagat.*, Vol. 13, 334–341, 1965.

13. Hasan M. A., and P. L. E. Uslenghi, "Electromagnetic scattering from nonlinear anisotropic cylinders - Part I: Fundamental frequency," *IEEE Trans. on Antennas Propagat.*, Vol. 38, 523–533, 1990.
14. Censor D., "Scattering by weakly nonlinear objects," *SIAM J. Appl. Math.*, vol. 43, 1400–1417, 1983.
15. Slaney, M., A. C. Kak, and L. E. Larsen, "Limitations of imaging with first-order diffraction tomography," *IEEE Trans. Microwave Theory Tech.*, Vol. MTT-32, 860–873, 1984.